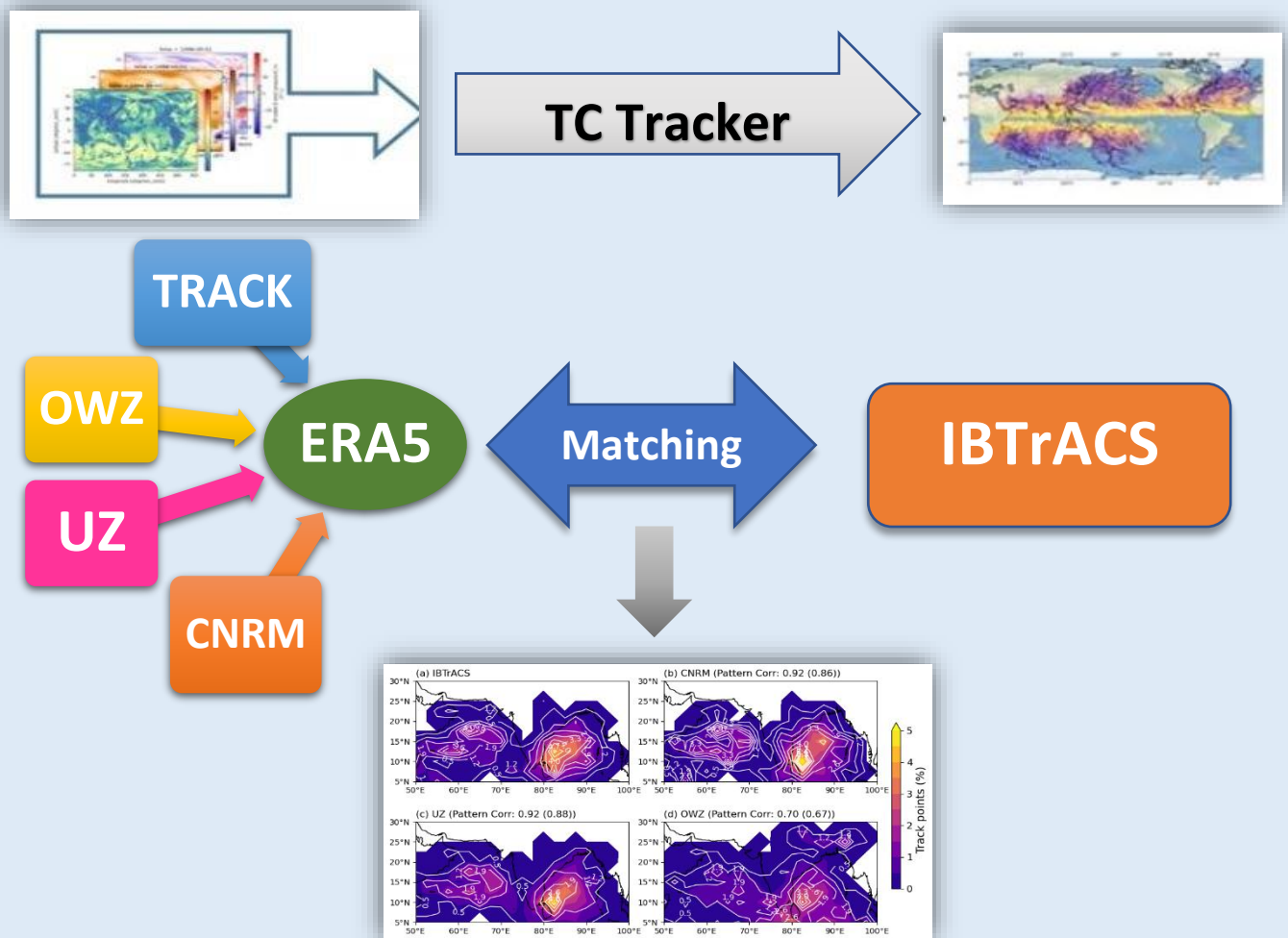


Assessment of Tropical cyclone tracking algorithms for the north Indian Ocean

Rushikesh Adsul, Vineet Kumar Singh, Anant Parekh and C. Gnanaseelan



Indian Institute of Tropical Meteorology (IITM)
Ministry of Earth Sciences (MoES)
PUNE-411008, INDIA

<https://www.tropmet.res.in/>

Assessment of Tropical cyclone tracking algorithms for the north Indian Ocean

Rushikesh Adsul, Vineet Kumar Singh, Anant Parekh and C. Gnanaseelan*

Climate Variability and Prediction, Indian Institute of Tropical Meteorology, Ministry of
Earth Sciences, Pune 411 008 India

***Corresponding Author:**

Dr. C. Gnanaseelan
Scientist G and Project Director
Climate Variability and Prediction (CVP)
Indian Institute of Tropical Meteorology,
Dr. Homi Bhabha Road, Pashan, Pune-411 008, India.
E-mail: seelan@tropmet.res.in
Phone: +91 -(0)20-259 04 271



Indian Institute of Tropical Meteorology (IITM)
Ministry of Earth Sciences (MoES)
PUNE, INDIA

<https://www.tropmet.res.in/>

DOCUMENT CONTROL SHEET

Ministry of Earth Sciences (MoES)
Indian Institute of Tropical Meteorology (IITM)

ESSO Document Number

ESSO/IITM/CVP/TR/01(2026)/205

Title of the Report

Assessment of Tropical cyclone tracking algorithms for the north Indian Ocean

Authors

Rushikesh Adsul, Vineet Kumar Singh, Anant Parekh and C. Gnanaseelan

Reviewers

Dr. A. K. Sahai

[Indian Institute of Tropical Meteorology, Pune]

Dr Medha Deshpande

[Indian Institute of Tropical Meteorology, Pune]

Dr. Vishnu S. Nair

[Indian Institute of Science Education and Research, Thiruvananthapuram]

Type of Document

Technical Report

Number of pages and figures

31, 10

Number of references

55

Keywords

Tropical cyclone, Cyclone Tracking Algorithms, north Indian Ocean, Post Monsoon

Security classification

Open

Distribution

Unrestricted

Date of Publication

February 2026

Abstract

Reanalysis datasets are widely used to assess the local and large-scale ocean-atmospheric conditions that impact the tropical cyclones characteristics. However, the tracking of tropical cyclones using the reanalysis in the different ocean basins is still debatable. In this study, we have demonstrated that the tropical cyclone detection and their tracking using different algorithms display significant variations in the north Indian Ocean based on ERA5 reanalysis data ($0.25^\circ \times 0.25^\circ$, 6 hourly) for the period 1990–2022. Comparison of observed tropical cyclones with reanalysis reveals that, among the tested algorithms (UZ, CNRM, OWZ, and TRACK), the CNRM algorithm outperforms UZ and OWZ and provides a realistic representation of TC tracks, with an approximate probability of detection of 80%. In contrast, the TRACK algorithm substantially overestimates TC occurrences relative to observations. Additionally, the track error in the reanalysis, relative to observations, is less than 50 km for approximately 65% of TC points. CNRM tracker performs better in the accurate representation of the spatial distribution and interannual variability of TC frequency, and TC duration. Given the fact that TC metrics are highly sensitive to the choice of tracker, this study identifies CNRM algorithm as the most effective tracking tool for the north Indian Ocean. This makes it a reliable method for TC detection and tracking in reanalysis datasets and climate models, with implications for future projections.

Summary

This study evaluates the performance of multiple tropical cyclone (TC) tracking algorithms over the North Indian Ocean (NIO) using the ERA5 reanalysis dataset ($0.25^\circ \times 0.25^\circ$, 6-hourly) for the period 1990–2022. Four algorithms—CNRM, UZ, OWZ, and TRACK—were assessed against observed TC records to quantify detection skill and track accuracy. Substantial differences were found among the trackers. The CNRM algorithm shows the best overall performance, achieving an approximate probability of detection of ~80% and providing the most realistic representation of TC tracks. Around 65% of TC track points exhibit spatial errors of less than 50 km relative to observations. CNRM also more accurately captures the spatial distribution, interannual variability, and duration of TCs over the NIO. In contrast, the TRACK algorithm considerably overestimates TC frequency compared to observations, while UZ and OWZ show lower detection skill.

The results highlight the strong sensitivity of TC metrics to tracker choice and identify CNRM as the most reliable tool for TC studies in the NIO.

Contents

1. Introduction	1
2. Data and Methodology	4
2.1 Data	4
2.1.1 TC and Reanalysis data	4
2.2 TC detection methodology	4
2.2.1 Tempest Extremes software	5
2.2.2 UZ algorithm	5
2.2.3 OWZ algorithm	6
2.2.4 CNRM algorithm	7
2.2.5 TRACK algorithm	7
2.2.6 Tracks matching algorithm:	8
3. Results	9
3.1 Climatology of TCs in observation	9
3.2. TC track distribution and detection	11
3.3 TC duration and track error	16
4. Discussion and Conclusion	22
Acknowledgement	25
References	26

1. Introduction

Tropical cyclone (TC) is one of the most severe extreme events, which causes great economic, environmental and societal impact. This is mainly due to their capacity to encompass various hazards such as strong wind (Zhou et al., 2018), heavy rainfall (Gaona et al., 2018), and storm surge within a span of 1 or 2 days (Chand & Walsh, 2012). The relatively short observational record of TCs and issues with sampling within that record contribute to significant uncertainty in various TC characteristics such as its frequency and intensity. Due to this uncertainty, it becomes difficult for the scientific community to evaluate the long-term variability and trends associated with TCs. However, the utilization of various reanalysis for TC detection presents an opportunity to mitigate this uncertainty (Truchelut et al., 2013). Additionally, TCs within reanalysis datasets often serve as a benchmark for observational assessments and calibration of simulated TCs by general circulation models (Bell et al., 2013; Murakami & Sugi, 2010; Rathmann et al., 2014; Strachan et al., 2013). However, the representation of TC characteristic in the reanalysis dataset depends on the reanalysis model dynamical core, parameterizations (Murakami, 2014), and its resolution (K. Hodges et al., 2017). Nevertheless, an unbiased representation of TCs in reanalysis is also very crucial for an improved understanding of the interaction between the climate system and TCs (Scoccimarro et al., 2012).

Several studies in different ocean basins are carried out to detect the TCs in the reanalysis datasets using various TC tracking algorithms (Bourdin et al., 2022; Hodges et al., 2017; Murakami et al., 2014; Zarzycki et al., 2021). There are two ways to detect TCs in the reanalysis datasets. First one is the physics-based trackers and second is the dynamic-based trackers. The physics-based trackers are based on the detection of a local minimum sea level pressure along with an anomalous warm-core criterion in the atmospheric column (Camargo & Zebiak, 2002; Chauvin et al., 2006, hereafter CNRM; Zarzycki & Ullrich, 2017, hereafter UZ). Further, an intensity criterion is applied based on the near surface wind speed and vorticity. On the other hand, the dynamic trackers track TCs mainly by using the dynamic variables such as vorticity or some derivatives of velocity. Using this dynamic approach, a TRACK method and Obuko-Weiss-Zeta (OWZ) algorithm is developed (Hodges et al., 2017; Tory et al., 2013). The advantage of dynamic tracker is that it is mainly resolution independent, thus can be used for inter-comparison between various reanalysis datasets (Tory et al., 2013).

Using the above-mentioned two methods, previous studies have proposed different thresholds based on near surface wind speed, vorticity and temperature anomalies to track the TCs in the reanalysis datasets and climate models (Albert et al., 2021; Bell et al., 2018; Camargo & Zebiak, 2002; Jin et al., 2016; Murakami et al., 2012, 2014; Oouchi et al., 2006). Oouchi et al. (2006) used the 850 hPa relative vorticity threshold along with thresholds of wind speed, surface pressure and temperature anomalies to detect TC. Similarly, Murakami et al. (2012) used 850 hPa relative vorticity, warm-core structure and temperature anomaly thresholds to detect TC. Whereas Camargo & Zebiak (2002) proposed basin and model dependent threshold criteria in atmospheric general circulation models. Using the OWZ scheme, Bell et al. (2018) evaluated the TC track climatology in ERA-Interim reanalysis and compared with the observations, they noted that this algorithm realistically captures the track of TCs.

Despite the availability of various TC tracking methods, only a few studies have carried out a comparison between various TC algorithms. A comparison done by Horn et al. (2014) show that the physics-based trackers gave significantly different results mainly due to the differences in the thresholds used to detect TCs. Raavi & Walsh (2020) subsequently conducted a comparative analysis between the Commonwealth Scientific and Industrial Research Organisation (CSIRO) and OWZ trackers. Their findings revealed that the OWZ tracker yielded better outcomes across various resolutions, whereas the CSIRO tracker has good performance with high-resolution datasets. Bourdin et al. (2022) carried out a global comparison of various TC tracking algorithms and they concluded that even the dynamic trackers gave inconsistent TC days in different ocean basins with mean TC duration smaller than the observation for UZ and CNRM and longer for TRACK. Due to the existing differences among different TC tracking algorithms, it is impossible to have a fair comparison between different studies. To address this issue and ensure a fair and reproducible assessment, the present study focuses on a carefully selected set of TC tracking algorithms. We employ the CNRM, UZ, TRACK, and OWZ trackers, which have been systematically evaluated together within a unified framework by Bourdin et al. (2022), providing a consistent benchmark for intercomparison. These algorithms collectively represent the two dominant TC tracking paradigms, namely physics-based approaches (CNRM and UZ) and dynamics-based approaches (TRACK and OWZ). By restricting the analysis to this well-documented and methodologically diverse set of trackers, we aim to minimize structural inconsistencies and facilitate a more robust comparison of TC characteristics

The north Indian Ocean (NIO) (comprising the Arabian Sea (AS) and the Bay of Bengal (BoB)) accounts for only about 6% of the annual global TC frequency (e.g., Singh & Roxy, (2022)). Despite the relatively low number of TCs compared to the global average, this basin is known to produce some of the deadliest storms due to its densely populated coastal regions (Chowdhury et al., 1993; Emanuel, 2005). TC activity in the NIO primarily occurs during two seasons: the pre-monsoon (April to early June) and the post-monsoon (October to December) periods (e.g., Singh & Roxy (2022)). As shown in figure 1a, TC activity during the post-monsoon season is nearly twice as high as that during the pre-monsoon season.

Bourdin et al. (2022) highlight that existing TC detection algorithms in this region often perform poorly in accurately capturing TC characteristics. This reduced performance is primarily associated with the nature of North Indian Ocean cyclones, which are frequently weak, short-lived, and embedded within monsoon-related disturbances, making it challenging for standard tracking algorithms to consistently distinguish true TCs from monsoon lows. This limitation arises mainly from the characteristics of the storm environment rather than from uncertainties in the underlying reanalysis datasets. However, their analysis was limited to annual TC statistics, without distinguishing between seasonal variations. In reality, the pre- and post-monsoon TC seasons are influenced by distinct ocean-atmosphere conditions, which significantly affect TC characteristics (Singh & Roxy, 2022). While these seasonal changes modify the background large-scale flow, the fundamental dynamical features used for TC detection—such as closed circulation, a vorticity maximum, a pressure minimum, and a warm-core structure—remain intrinsic to tropical cyclones. Therefore, it is crucial to evaluate how various TC detection algorithms perform during each season individually. Given the higher frequency of TCs during the post-monsoon season, their more frequent landfall over the east coast of India as compared to the pre-monsoon season, and the lack of detailed, season-specific evaluations of TC detection methods, this study aims to conduct a comprehensive comparison of the performance of different TC detection trackers in the NIO, specifically for the post-monsoon season. The comparison is carried out by assessing the TC tracks detected by these algorithms using ERA5 reanalysis data (Hersbach et al., 2020), and validating them against the best track data from the India Meteorological Department (IMD), as archived in the International Best Track Archive for Climate Stewardship (IBTrACS; (Knapp et al., 2010)). However, we acknowledge that ERA5 exhibits known limitations in representing tropical cyclone wind intensities, as highlighted by recent assessments (e.g., Liu et al., 2025).

This paper is organised as follows: Section 2 encompasses a detailed discussion of the algorithms of different TC trackers and the datasets and methodology employed. Section 3 delves into the study's findings and provides a comprehensive analysis of the best performing TC tracker. The conclusion of the study is presented in Section 4.

2. Data and Methodology

2.1 Data

2.1.1 TC and Reanalysis data

We have carried out analysis of NIO TCs in the post-monsoon season (October-December) for the period 1990–2022. For this analysis, the TC data is obtained from IMD (IMD 2021) as archived in the IBTrACS dataset (Knapp et al., 2010). The above-mentioned period is chosen due to the limited availability of the NIO TC maximum wind speed data in the IBTrACS database. Only those systems that have reached the tropical storm intensity that is having a maximum wind speed of at least 34 knots are considered (Deng et al., 2025). To identify and track TCs in the reanalysis dataset, we have obtained atmospheric variables (mean sea level pressure, u-wind, v-wind, relative vorticity and air temperature) from the fifth generation of ECMWF Reanalysis (ERA5) dataset (Hersbach et al., 2020) at a spatial resolution of $0.25^\circ \times 0.25^\circ$. The reanalysis data is obtained at a temporal resolution of 6 hours in order to maintain consistency with the TC data.

In contrast to other reanalysis products, such as JRA-55 and NCEP-CFSR, ERA5 does not incorporate targeted tropical cyclone assimilation procedures (Hodges et al., 2017). Nonetheless, recent evaluations have demonstrated that ERA5 performs comparably better than JRA-55 and NCEP-CFSR across a range of cyclone metrics (Zarzycki et al., 2021), where tropical cyclones were identified using the UZ tracking algorithm. For this reason, ERA5 was selected as a consistent reference to link observations and simulations, with the primary aim of comparing the detection skill of four tropical cyclone tracking algorithms.

2.2 TC detection methodology

TC trackers are algorithms which detect cyclonic systems associated with a warm core in a gridded dataset and link them together into a track. The methodology adapted for detection of TCs in different tracking algorithms is discussed below:

2.2.1 Tempest Extremes software

Tempest Extremes (see <https://climate.ucdavis.edu/tempestextremes.php>) is a command-line software which is used for fast and versatile implementation of TC trackers. It has been developed by Zarzycki & Ullrich (2017). This algorithm provides two functions Detect Nodes and Stitch Nodes respectively for tracking of pointwise features like TCs. Detect Nodes identifies candidate "nodes" that match the local extrema of a given variable and may also meet a set of further requirements such as thresholds, closed contours, etc. and Stitch Nodes creates a track by connecting candidates within a given radius of each other. In this research, we used the Tempest Extremes software to implement two TC trackers—UZ, described by Ullrich et al. (2021) and OWZ, described by Tory et al. (2013).

2.2.2 UZ algorithm

It is physics-based algorithm and the thresholds used in this algorithm to detect TC are computed by Zarzycki & Ullrich (2017) using sensitivity analysis to several metrics from different reanalysis products. It includes two stages viz. candidate detection and stitching TC tracks. For candidate detection firstly local minima of sea level pressure are identified. It gives several candidate points and out of these candidate points only those points are retained which satisfy the following conditions:

1. Over a 5.5° great-circle distance from the candidate point, sea level pressure must increase by 2 hPa.
2. The geopotential thickness between 300 hPa and 500 hPa (or $Z_{300-500}$), must drop by $58.8 \text{ m}^2\text{s}^{-2}$ over a distance of 6.5° great circle distance, using the maximum value of $Z_{300-500}$ within 1° great circle distance of the minimum sea level pressure as a reference.

These two criteria are applied to ensure that the low-pressure area is strong and has an upper-level warm core.

After candidate detection, consecutive candidates are linked together if they lie within 8° great circle distance of one another. A gap of maximum 24 hours is allowed in a track, and track duration must be ≥ 54 hours. Additional conditions must be satisfied by the ten 6-hourly time steps (54 h), these are: $U_{10} \geq 10 \text{ ms}^{-1}$; $|\phi| \leq 50^\circ$; $z_{\text{surf}} \leq 150 \text{ m}$, where U_{10} is the 10 minute near-surface sustained wind, ϕ and z denotes the latitude and altitude, respectively. These thresholds make sure that the track is long enough, it remained situated in the tropical areas and over ocean for a significant duration of its lifetime.

2.2.3 OWZ algorithm

The OWZ algorithm was first presented in Tory et al. (2013) and is slightly modified and implemented using Tempest Extremes framework by Bourdin et al. (2022). It is based on analysing the Obuko-Weiss-Zeta (OWZ) quantity, which is defined as

$$OWZ = \max(OW_{norm}, 0) \times \eta \times \text{sign}(f) \quad \text{-----}(1)$$

where η is the absolute vorticity, which is the sum of the relative vorticity ζ and the Coriolis parameter f , and OW_{norm} stands for the normalized Obuko-Weiss parameter:

$$OW_{norm} = \frac{\zeta^2 - (E^2 + F^2)}{\zeta^2} \quad \text{-----} (2)$$

where E and F are the stretching and the shearing deformation, respectively and are given by

$$E = \frac{\partial u}{\partial x} - \frac{\partial v}{\partial y}, F = \frac{\partial v}{\partial x} + \frac{\partial u}{\partial y} \quad \text{-----}(3)$$

For the candidate detection, we first identify the local maxima of OWZ at 850 hPa using our implementation of OWZ in Tempest Extremes. Candidates are excluded for which there is a stronger OWZ maximum within 5° great circle distance. The candidates are then limited to those which meet the following six requirements, which must be met within 2° great circle distance of that maximum:

- $OWZ_{850hPa} \geq 5 \times 10^{-5} \text{ s}^{-1}$
- $OWZ_{500hPa} \geq 4 \times 10^{-5} \text{ s}^{-1}$
- $r_{950hPa} \geq 70\%$
- $r_{700hPa} \geq 50\%$
- $q_{950hPa} \geq 10 \text{ g kg}^{-1}$
- $vws \leq 25 \text{ m s}^{-1}$

where r is the relative humidity, q is the specific humidity and vws is the vertical wind shear which is calculated as the vector difference of the horizontal winds between 200 and 850 hPa.

After candidate detection, consecutive points are linked together if they lie within 5° great circle distance of one another, allowing for a maximum 24 hour gap. Also, additional thresholds in the centre of the system must be met for at least 9 time-steps (48 hours). This additional thresholds for the centre of the system:

- $OWZ_{850hPa} \geq 6 \times 10^{-5} s^{-1}$
- $OWZ_{500hPa} \geq 5 \times 10^{-5} s^{-1}$
- $r_{950hPa} \geq 85\%$
- $r_{700hPa} \geq 70\%$
- $q_{950hPa} \geq 14 g kg^{-1}$
- $vws \leq 12.5 m s^{-1}$

Tracks are finally filtered out if they do not reach tropical storm intensity ($u_{10}=16 ms^{-1}$) for at least one time step.

2.2.4 CNRM algorithm

This algorithm was The CNRM tracker is named after the Centre National de Recherches Météorologiques, where the algorithm was originally developed by Chauvin et al. (2006) to track TC.

In this algorithm the following criteria are used to track the TC:

1. The sea level pressure must be lower than surrounding, the region of pressure minimum indicates the system's centre.
2. $\zeta_{850 hPa} \geq 1.5 \times 10^{-4} s^{-1}$.
3. $U_{850 hPa} \geq 5 m s^{-1}$.
4. The sum of the temperature anomalies averaged over the 700, 500, 300 hPa pressure levels $\geq 1 K$.
5. Difference in temperature anomaly (850 hPa minus 300 hPa) $\leq 1 K$.
6. Difference in wind speed (300 hPa minus 850 hPa) $\leq 5 m s^{-1}$.

The TC which has a lifespan of less than 1 day are not considered in this study.

2.2.5 TRACK algorithm

The TRACK algorithm is designed to track all the relative vorticity perturbation areas, as a result it can detect both extratropical cyclones and TCs (Hodges, 1994). In order to remove the extratropical cyclones a warm core criterion is applied in the final stage of the TRACK algorithm. The algorithm is based on $\zeta_{T63}(P)$ which is the relative vorticity at pressure level P, spectrally filtered to retain total wavenumbers 6-63 only, also it is vertically averaged from 850

to 600 hPa called as avg ζ_{T63} . The candidate points are detected based on criteria $\text{avg } \zeta_{T63} > 5 \times 10^{-6} \text{ s}^{-1}$. The candidate points are then connected by minimizing a cost function to ensure track smoothness, as described by (Hodges, 1995, 1999). The resulting tracks must persist for at least two days and the first detected candidate point must be between latitudes 30°S and 30°N.

Additional criteria to filter out only the warm core systems is applied using the following criteria:

1. $\zeta_{T63} (850 \text{ hPa}) > 6 \times 10^{-5} \text{ s}^{-1}$.
2. $\zeta_{T63} (850 \text{ hPa}) - \zeta_{T63} (250 \text{ hPa}) > 6 \times 10^{-5} \text{ s}^{-1}$.
3. Local maxima of ζ_{T63} must exist at each pressure level.

2.2.6 Tracks matching algorithm:

In order to match the detected tracks by different tracking algorithm in the ERA5 with the observed TC track, we have adopted the following algorithm (Bourdin et al., 2022). Consider a given detected track ‘D’ having n points (d_1, d_2, \dots, d_n) at times (t_1, t_2, \dots, t_n). The observations ‘O’ consist of a database of tracks with track position and time. The points of ‘O’ at time t_i that are located closer than 300 km from the point d_i are associated with each point $d_i(t_i)$ of track ‘D’. The subset of points of ‘O’ that have been associated with any point in ‘D’ is denoted as $O_{D\text{-paired}}$. It is composed of $|O_{D\text{-paired}}|$ elements. If the points of ‘O’ at time t_i are greater than 300 km from the point d_i , then that point is not associated with the detected track ‘D’. This leads to three possible outcomes:

1. $|O_{D\text{-paired}}| = 0$: None of the points of ‘D’ is paired to a point in ‘O’, therefore, ‘D’ is considered as a false alarm (FA).
2. $|O_{D\text{-paired}}| > 0$ and all the points in $O_{D\text{-paired}}$ belong to the same track D_O in ‘O’: D_O is considered as a match of ‘D’.
3. $|O_{D\text{-paired}}| > 0$ and the points in $O_{D\text{-paired}}$ belong to more than one track in ‘O’: the observed track having the largest number of points paired with ‘D’ is considered the match of ‘D’.

If an observed TC track is paired with two or more detected TC track in the ERA5, then that detected track in ERA5 is merged into a single TC track. Such scenario happens when TC temporarily weakened for few hours and re-intensified later. Using this process we have categorized the TC tracks in three categories. First is Hits (H), which denotes the TC track detected in ERA5 and is also present in the observation. Second category is Misses (M), which denote the TC tracks which are present in observation but are not detected by the tracking algorithm in the ERA5. The third category is the False Alarm (FA), it denotes the TC tracks which are detected by the algorithm in the ERA5 but those TC tracks are not present in the observation. Based on the above-mentioned categories, two detection skills metrics are defined. These are the Probability of Detection (POD, also called as “Hit Rate (HR)”) and is given by equation 4,

$$POD(HR) = \frac{H}{H+M} \quad \text{-----} \quad (4)$$

Whereas, the False Alarm Rate (FAR) and is given by equation 5 (Barnes et al., 2009)

$$FAR = \frac{FA}{H+FA} \quad \text{-----} \quad (5)$$

It is to be noted that we have not carried out the post-processing procedure, as this is only required to filter out extra-tropical cyclones and other mid-latitude systems that might have been falsely detected by the tracking algorithms. Since the TC detection tracker is applied only up to 30°N, which covers the northern extent of NIO, no extra-tropical systems will be falsely detected by the algorithms.

3. Results

3.1 Climatology of TCs in observation

We have analyzed the TCs in the NIO during the period 1990–2022 using observational best-track data from IBTrACS, when on an average 4 TCs/year are formed in the NIO (Figure 1). Out of the total number of TCs, most of the TCs (~86%) have formed in the pre-monsoon (April–early June) and the post-monsoon (October–December) seasons (Figure 1). Thus, these two seasons are the main TC seasons in this basin which is in line with previous studies (e.g. Ali, 1999; Rajeevan et al., 2013; Sahoo & Bhaskaran, 2016; Singh et al., 2000). As mentioned earlier in the introduction, it can be seen from Figure 1 that out of the two TC seasons, the number of TCs in the pre-monsoon season in the NIO is significantly less ($p <$

0.01) compared to the post-monsoon season (which accounts for 63% of the annual TC formation in NIO). In the NIO, as compared to the pre-monsoon season, the TC distribution during the post-monsoon season is more of non-uniform between the AS and the BoB. During the post-monsoon season, the BoB basin hosts ~ 2 TCs/year, whereas in the AS the TC frequency is only 0.5 TC/year in the analysis period. The higher activity of TC in the BoB as compared to AS during the post-monsoon season is associated with the more favourable ocean-atmospheric conditions for the genesis of TC in this basin along with the re-intensification of remnants of TCs of west Pacific which travel westwards as a low pressure into the BoB (Singh & Roxy, 2022).

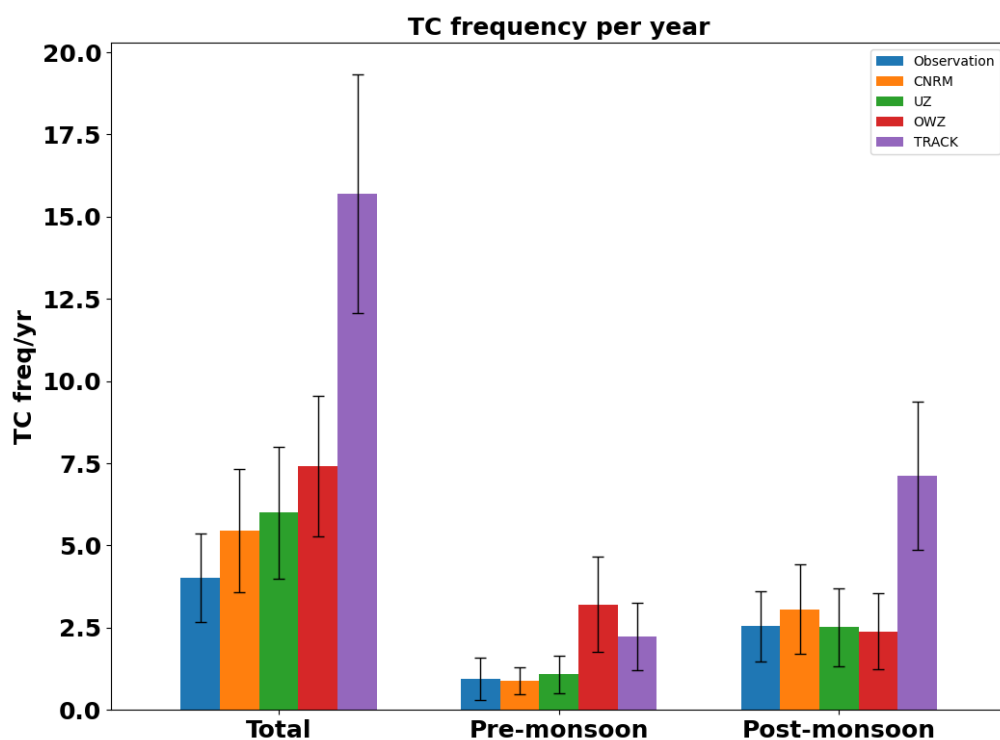


Figure 1. TC frequency per year in the North Indian Ocean (including the Arabian Sea and the Bay of Bengal) in observation (IBTrACS, blue), and ERA5 as detected by CNRM algorithm (orange), UZ algorithm (green), OWZ algorithm (red) and TRACK algorithm (purple) for the entire year as denoted by Total and pre-monsoon (April–June) and post-monsoon (October–December) seasons respectively for the period 1990–2022. The vertical lines denote one standard deviation in the TC frequency.

In order to see the spatial distribution of TC tracks in the NIO, we have analyzed the TC track density. Here tracks are plotted only for the timesteps when the system in the IBTrACS has at least a wind speed of 35 knots. From the track density figure 2a, we see that the TCs originating in the BoB mainly impact the coastlines of east India, Bangladesh, Sri Lanka and Myanmar (e.g., (Singh et al., 2000, Adsul et. al., 2026)) with maximum TCs hitting

the Andhra Pradesh and Tamil Nadu coast of India. Whereas, TCs in the AS mainly impact the coastlines of western India, Oman, Yemen and Pakistan (Figure 2a). Additionally, Figure 2a illustrates that a significant number of post-monsoon TCs exhibit a north westward/westward movement in both the AS and the BoB basin.

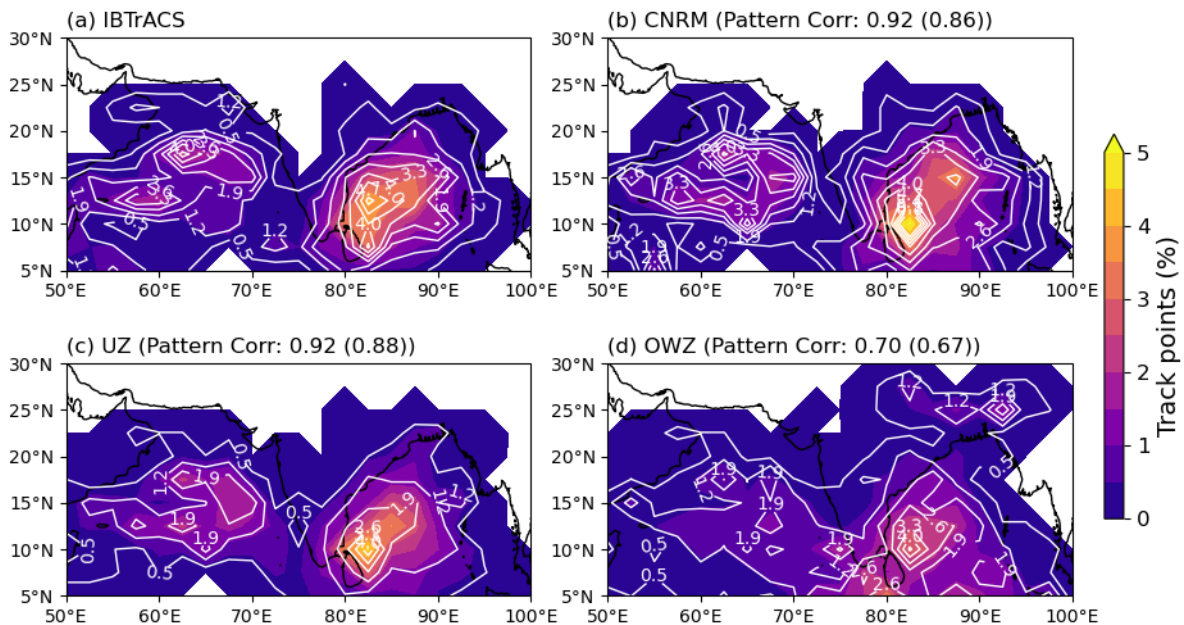


Figure 2. Percentage TC track density (shaded) and standard deviation of TC tracks (contour lines) for the post-monsoon season in (a) IBTrACS and (b-d) ERA5 using (b) CNRM (c) UZ (d) OWZ TC tracking algorithms for the period 1990–2022. Bracket and non-bracket values in (b-d) denote the pattern correlation of the TC track standard deviation and TC track density respectively between IBTrACS and ERA5 by using different TC tracking algorithms.

3.2. TC track distribution and detection

In the ERA5, all the TC tracking algorithms are over-estimating the annual frequency of TCs in the NIO (Figure 1). The CNRM and UZ algorithms are roughly detecting 30% and 39.3% more TCs than observed, whereas the OWZ algorithm is detecting almost double the TC frequency compared to observation. The overestimation of the UZ algorithm compared to the CNRM is mainly because of overestimation of TCs in the monsoon season (July–September). Among all the algorithms, the TRACK algorithm showed least skill, as it is overestimating the TC frequency by four times compared to the observation. This is similar to the findings of Bourdin et al. (2022) where they showed that TRACK algorithm overestimates the TC frequency over the globe. A season wise analysis shows that all the algorithms (except OWZ) are capturing the seasonal differences in the TC frequency with higher TC frequency in

the post-monsoon season compared to the pre-monsoon season. From the observation and ERA5 reanalysis it can be seen that the number of NIO TCs is more in the post-monsoon season than pre-monsoon season. The present analysis therefore focuses on post-monsoon TCs, as this season provides a substantially larger sample size, enabling more robust statistical assessment of tracker performance. In addition, a larger fraction of post-monsoon TCs make landfall, making this period particularly relevant for impact-oriented analyses. Pre-monsoon TCs, which exhibit distinct dynamical characteristics, are beyond the scope of the present study and will be examined separately in future work. During the post-monsoon season, the CNRM algorithm is overestimating the TC frequency by roughly ~19% and the OWZ algorithm is underestimating the TC frequency by ~6%. On the other hand, the UZ algorithm closely captures the observed TC frequency.

It is noted that the OWZ tracker identifies a higher number of pre-monsoon TC-like systems compared to the post-monsoon season, in contrast to observations and ERA5. This behavior reflects the diagnostic design of OWZ, which detects vorticity-rich, dynamically favorable disturbances rather than systems that necessarily intensify into observed tropical cyclones. During the pre-monsoon season, enhanced surface heating and stronger cross-equatorial flow increase low-level cyclonic vorticity over the NIO. Due to its high sensitivity to vorticity gradients, OWZ therefore flags a larger number of disturbances, many of which do not subsequently develop into mature cyclones.

Furthermore, consistent with the annual frequency, the TRACK algorithm significantly overestimates TC frequency during the post-monsoon season (Figure 1). This overestimation arises from TRACK's tendency to identify weak and short-lived low-pressure systems as tropical cyclones. Such systems occur more frequently during the post-monsoon period, when background low-level vorticity and synoptic disturbances are enhanced over the North Indian Ocean. As a result, TRACK retains a larger number of marginal systems that do not intensify into observed tropical cyclones, leading to higher TC counts compared to observations. Due to its unrealistic representation of TC climatology, the TRACK algorithm has been excluded from further analysis.

The spatial climatology of TCs is important given the highly regionalized nature of TC impacts within a basin. In the NIO, the CNRM and UZ algorithms efficiently capture the spatial distribution of the TC track density (pattern correlation of 0.92). A sub-basin analysis shows

that in the BoB, both the algorithms capture the maxima in TC track density near the southeast coast of India (Figure 2b, 2c). Similarly, in the AS, the maximum TC track density is realistically captured in the central AS. On the other hand, the OWZ algorithm also captures the maxima in TC track density in the southeast BoB, however, it significantly over-estimates the TC tracks in specific inland regions, particularly along the Odisha–West Bengal coast, parts of eastern India, Bangladesh, and land is high. On the other hand, in the AS, the OWZ algorithm shows a double maximum in TC track Myanmar (Figure 2d). This indicates that using the OWZ, the TCs in the ERA reanalysis is either penetrating more inland or false rate of this algorithm in capturing TC formation over the density, one at the Kerala coast (7°N-12°N, 73°E-76°E,) and other in the south-central AS (10°N-15°N, 60°E-70°E). Overall, in the AS there is a southward shift in the detected TCs as compared to the observation. Thus, in the NIO as a whole the [\[02106\]](#) in the sense that their study showed ERA5 reproduces realistic global TC track density patterns— including over the Indian Ocean—when evaluated using the UZ tracker. While Zarzycki et al. (2021) did not examine pre- and post-monsoon seasons separately or compare multiple algorithms as done here, their findings support the broader robustness of ERA5-based TC track density.

Similar to the TC track density pattern, the CNRM and UZ algorithms capture the interannual variability in TC tracks with a pattern correlation of 0.86 and 0.87 respectively, as shown in the standard deviation contours in Figure 2. Whereas, the interannual variability of TC tracks as captured by the OWZ algorithm is having a pattern correlation of only 0.67 with the observation. Based on the spatial pattern of TC tracks, variance, root mean square error of TC tracks and bias, we analyzed the Taylor skill score of each algorithm similar to Zarzycki et al. (2021). The Taylor diagram and Taylor skill score are useful tools as it combines multiple metrics to give a complete assessment in relation to a reference dataset (Taylor, 2001). The algorithms which have higher correlations with observation and have similar variance have low root mean square error and high Taylor skill score which varies in the range 0.0 (no skill) to 1.0 (perfect skill). Our analysis shows that CNRM has the highest skill of ~0.9 in capturing the TC tracks distribution and their interannual variability (Figure 3a-c). Whereas, the UZ algorithm has a Taylor skill score of 0.80 and 0.75 in capturing the TC track density and TC tracks variability respectively (Figure 3c). Thus, the CNRM algorithm displays the highest skill in capturing the track of TCs in this basin.

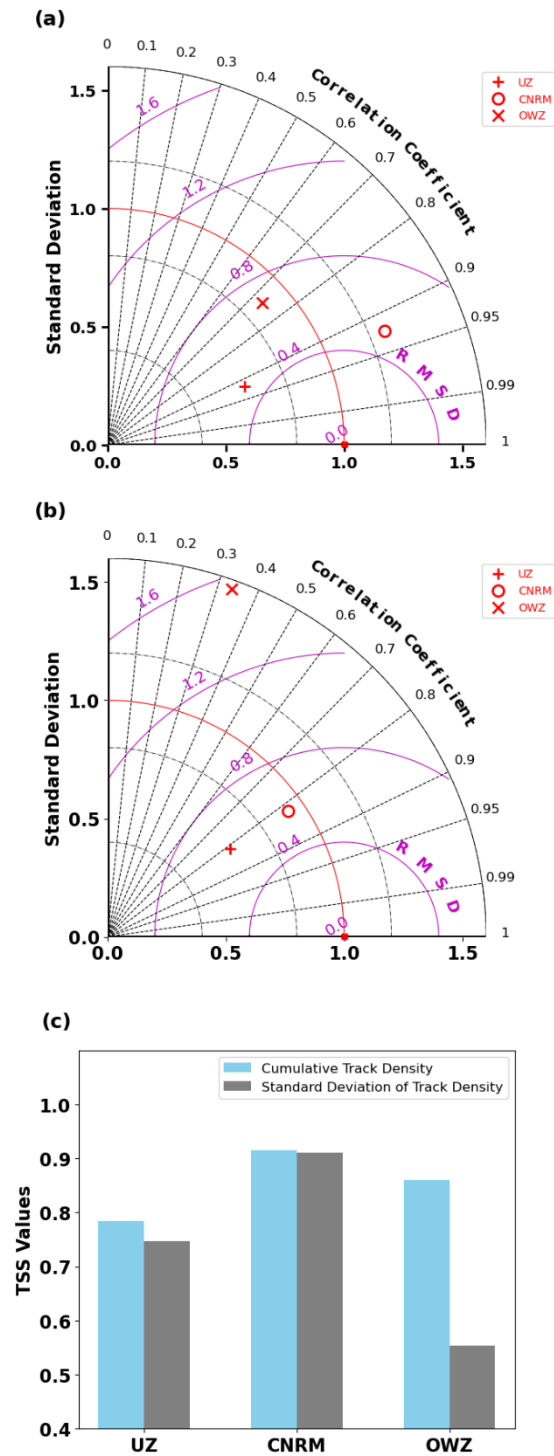


Figure 3. Taylor diagrams showing the performance of different tracking algorithms during the post-monsoon season over the North Indian Ocean for the period 1990–2022: (a) cumulative TC track density, (b) spatial standard deviation of TC track density, and (c) Taylor skill score (TSS).

Using equations 4 and 5 we also evaluated the TC tracks which are falsely detected by the tracking algorithm. For the NIO as a whole, CNRM algorithm captures ~78% of the total observed tracks. Moreover, the POD for NIO is almost identical to the global POD of TCs

found by Zarzycki et al. (2021). On the other hand, POD of UZ and OWZ are 68% and ~62% respectively, which are less than that of CNRM (Figure 4a). It is also important to mention that the TCs missed by CNRM are mainly the weak TCs and the TCs that reached TC strength only for a short duration, this further strengthen the potential of CNRM. Murakami (2014) and Hodges et al. (2017) also shown that the Hit rate increases with the intensity of TC and the stronger TCs are more likely to be Hits in the tracking algorithm. There are sub-basin differences in the POD skill by the three different algorithms (Figure 4a). The POD by all the three algorithms in AS is lower compared to the BoB. Despite the differences between the two basins, the CNRM shows the highest POD in the BoB, while the UZ algorithm exhibits the highest POD in the AS (Figure 4a). The reason for the sub-basin differences in the POD by the different algorithms is beyond the scope of this study.

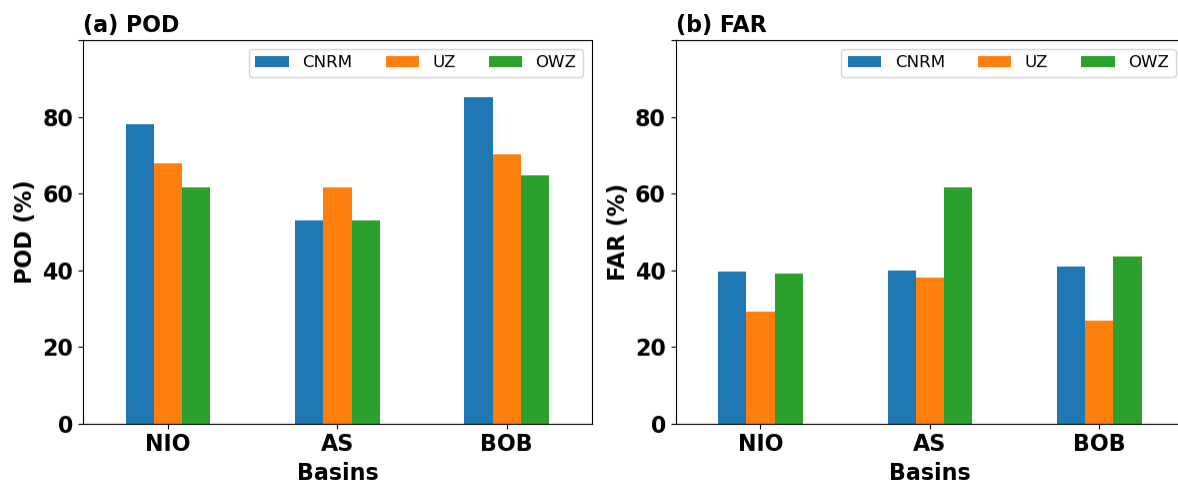


Figure 4. The distribution of (a) Probability of Detection (POD) and (b) False Alarm Rate (FAR) of the TCs in the North Indian Ocean as a whole and its sub-basins Arabian Sea (AS) and the Bengal (BoB) during the post-monsoon season in the ERA5 reanalysis dataset using CNRM (blue), UZ (orange) and OWZ (green) algorithms.

An analysis of FAR (Figure 4b) reveals that for the NIO, the two trackers that is CNRM and OWZ has similar FAR of 39.6% and 39.2% respectively, suggesting that 39-40% of the TC tracks are false in the CNRM and OWZ algorithm. On the other hand, UZ algorithm had the FAR of only 29.3% which is the lowest among all the three algorithms (Figure 4b). Sub-basin analysis reveals that for the CNRM unlike the POD, the FAR remains nearly the same in both the AS and the BoB. On the other hand, FAR for the UZ and OWZ algorithms are higher in the AS compared to the BoB (Figure 4b). A high FAR in CNRM as compared to UZ indicates that in the CNRM too many false TCs are detected. One plausible explanation for higher FAR in CNRM is the difference in the minimum duration threshold required to identify a TC.

3.3 TC duration and track error

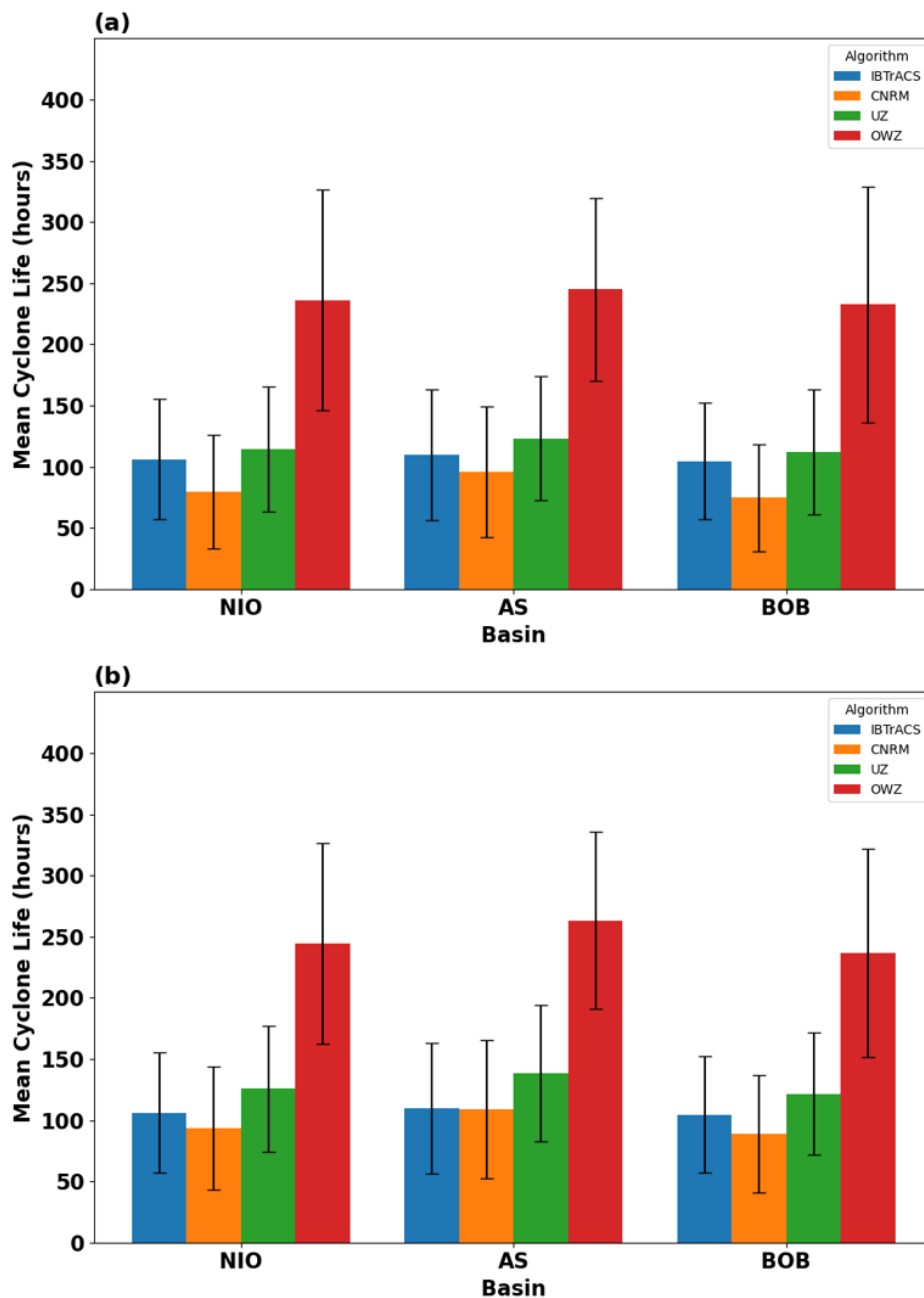


Figure 5. (a) Mean TC lifespan (hours) for all TCs (Hit and False Alarm) during the post-monsoon season in observation (IBTrACS, blue), and as detected in ERA5 by CNRM algorithm (orange), UZ algorithm (green) and OWZ algorithm (red) in the north Indian Ocean (NIO) as a whole and in sub-basins Arabian Sea (AS) and Bay of Bengal (BoB) separately. (b) Same as in (a) but TC lifespan only for those TCs which are Hit that is TC which are present in observation and are also detected by the algorithm.

We also analysed the TC lifespan in the NIO in both observation and in the reanalysis. The observed TC lifespan in NIO is computed from the genesis of a TC till its dissipation and also includes the timesteps when the system has winds less than 17 m s^{-1} . This methodology is adopted to have a fair comparison with the TC trackers used in the reanalysis, as the wind speed

thresholds in the TC trackers are less than 17 m s^{-1} . The average duration of TC in the NIO is 106.2 hours in IBTrACS and is nearly same for both the basins (Figure 5a). In the reanalysis first we analyzed the TC duration combining both the Hit and the FA. We found that in the NIO, CNRM underestimates the duration of TC by ~ 27 hours, and by ~ 14 hours and ~ 30 hours respectively for AS and BoB. The UZ on the other hand slightly over-estimate the TC duration by ~ 8 hrs in the NIO. The OWZ algorithm significantly over-estimate the TC duration in both the AS and BoB (Figure 5a). We conducted an additional analysis of the TC duration, focusing exclusively on Hits. Figure 5b shows that, after excluding false alarm TCs, the TC duration of CNRM has an error of only 1 hour in the AS and ~ 27 hours in the BoB compared to the total TCs detected by the algorithm (False Alarms + Hits). Overall, for the NIO, the TC duration increased by ~ 14 hours. Whereas, using the UZ algorithm, there was a ~ 15 hours increase in TC duration in the AS and ~ 10 hours increase in the BoB after removing false alarm TCs. Similarly, the OWZ also showed an increase (Figure 5b). The increase in TC duration after excluding false alarm TCs is primarily due to the fact that false alarm TCs in the reanalysis tend to be weaker and shorter-lived, resulting in a shorter duration compared to Hit TCs. Thus, removing false alarm TCs increases the mean TC duration as detected by all three algorithms. Furthermore, Figure 5b reveals that for Hits, among the three algorithms, the TC duration in the reanalysis has the least bias for CNRM in both the AS and the BoB. For the NIO as a whole, the CNRM exhibits a bias of only ~ 12 hours, whereas the UZ and OWZ show biases of ~ 20 hours and ~ 138 hours, respectively.

We further analyse the timing of detected tracks relative to IBTrACS by examining the delay in the first and last detected track points (Figure 6). The first-point delay (Figure 6a) quantifies how well each algorithm captures the onset of observed tracks, while the last-point delay (Figure 6b) reflects the ability to capture track termination. The results indicate that the CNRM algorithm exhibits minimal median delays and relatively narrow distributions for both the start and end points over the Arabian Sea and the Bay of Bengal, suggesting close temporal agreement with observations and a realistic representation of TC evolution. In contrast, the UZ algorithm tends to detect systems slightly earlier and to terminate them marginally later, leading to small negative first-point delays and modest positive last-point delays. The OWZ algorithm shows the largest timing biases, with pronounced negative first-point delays and positive last-point delays in both basins, indicating earlier detection and prolonged persistence of tracks relative to observations. Basin-wise, the timing delays are generally larger and more variable over the Arabian Sea than over the Bay of Bengal, particularly for UZ and OWZ,

reflecting greater uncertainty in capturing TC evolution over the Arabian Sea. Overall, this timing analysis provides a physical explanation for the TC duration biases discussed earlier and further highlights the superior performance of the CNRM algorithm in representing both TC genesis and dissipation stages.

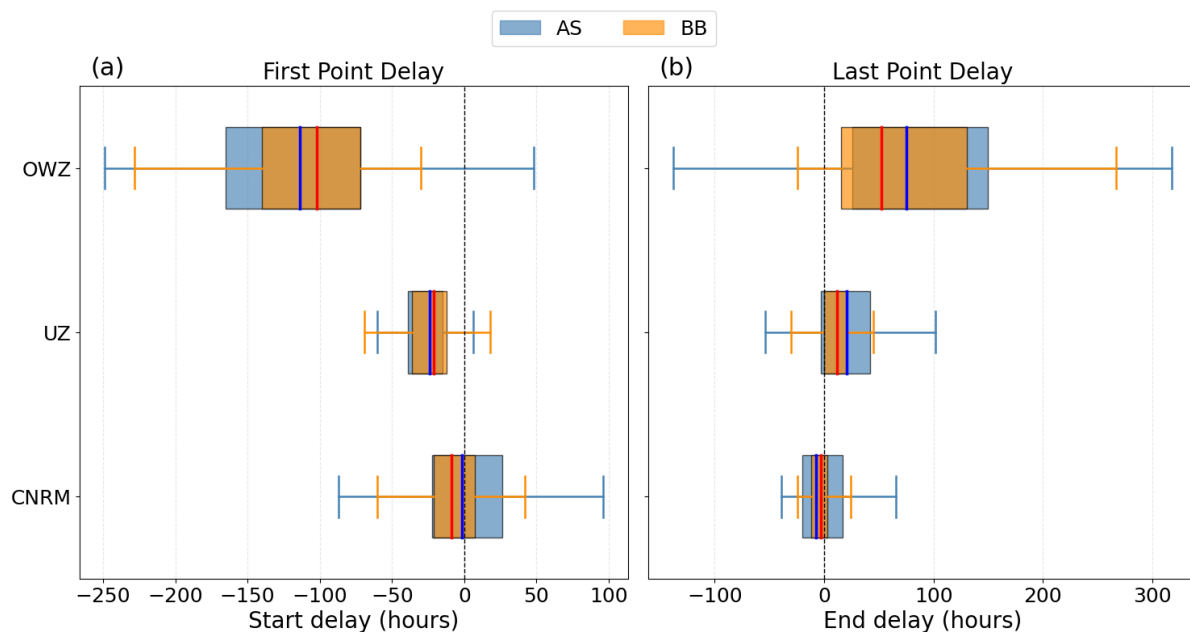


Figure 6. First- and last-point timing delays (hours) of algorithm-detected tropical cyclone tracks relative to IBTrACS over the Arabian Sea (AS) and Bay of Bengal (BB). Panel (a) shows the first-point delay, defined as the difference in track initiation timing, while panel (b) shows the last-point delay, defined as the difference in track termination timing. Negative (positive) values indicate earlier (later) detection compared to observations.

We further examined how different categories of detected systems—Hits, False Alarms (FA), and Misses—are distributed across tropical cyclone intensity, as represented by minimum sea-level pressure, for the three tracking algorithms over the NIO and its sub-basins, the Arabian Sea (AS) and the Bay of Bengal (BoB) (Figure 7). The results show that the CNRM algorithm consistently detects a larger fraction of intense tropical cyclones, particularly those with minimum central pressures below 985 hPa, with this behaviour being most prominent over the Arabian Sea (Figure 7a, d). This indicates a better capability of CNRM in identifying stronger systems. In addition, the mean lifetime of Hit cases in CNRM is systematically higher across pressure bins compared to both False Alarms and Misses, highlighting its ability to track long-lived and well-organized cyclones (Figure 7a, d, g). In contrast, the UZ and OWZ algorithms exhibit weaker separation between Hits and False Alarms in terms of both intensity and duration (Figure 7b–c, e–f, h–i). In particular, for the OWZ algorithm, a substantial fraction

of False Alarms is associated with relatively low central pressures and moderate lifetimes, indicating that several non-TC systems are misidentified as tropical cyclones. This behaviour suggests that OWZ tends to detect transient or weakly organized systems, such as monsoon lows, as TCs. These results are consistent with the findings of Bourdin et al. (2022), who showed that structure-based algorithms such as CNRM are more effective in identifying intense and long-lived cyclones, whereas vorticity-based approaches like OWZ are more prone to misclassifying weaker or short-lived systems. This overall behaviour is consistently observed over both the Arabian Sea and the Bay of Bengal (Figure 7c, f, i).

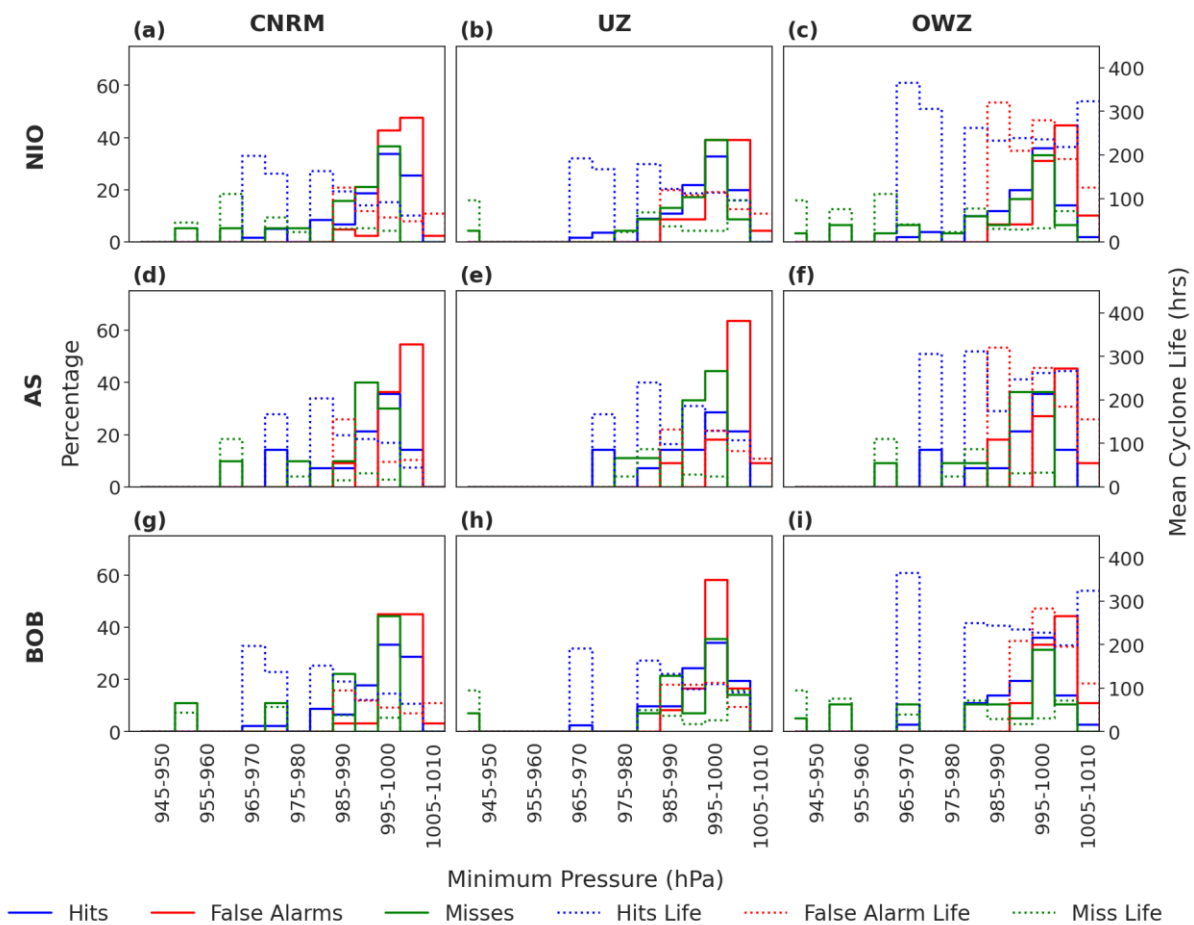


Figure 7. Stepped histograms of TC minimum sea-level pressure (MSLP, shown by thick bars) and corresponding mean cyclone lifespans (hours, shown by dash bars) for systems classified as Hits (blue), False Alarms (red), and Misses (green) by CNRM, UZ, and OWZ across the North Indian Ocean (NIO), including the Arabian Sea (AS) and Bay of Bengal (BOB).

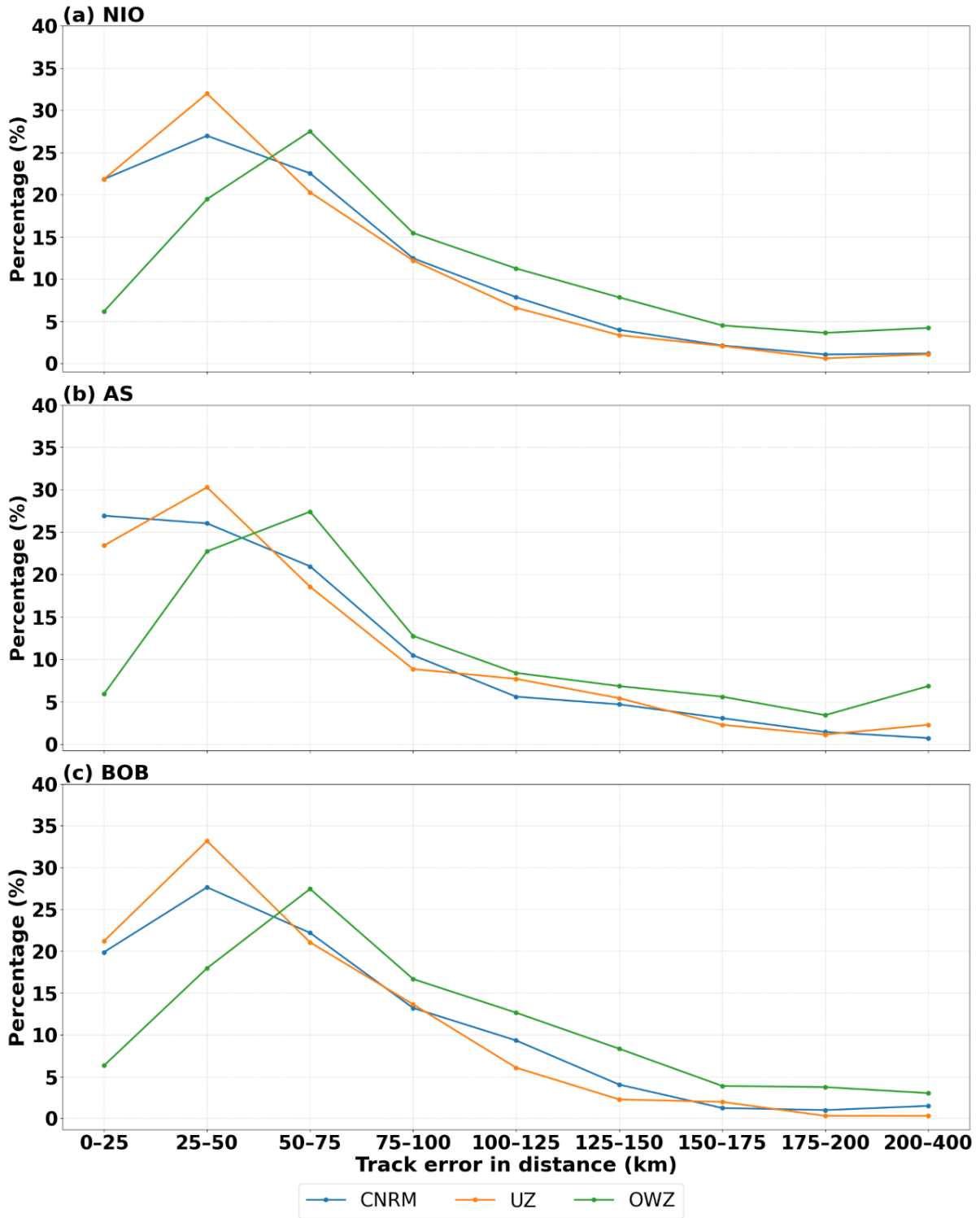


Figure 8. Composite of probability of TC track error distribution in the (a) north Indian Ocean (b) Arabian Sea and (c) Bay of Bengal in ERA5 using CNRM (blue), UZ (orange) and OWZ (green) algorithms during the post-monsoon season.

We also evaluated the best performing algorithm by assessing the TC track error with respect to the observation. In the reanalysis, an accurate representation of TC tracks with minimal error is crucial, as an error in the TC tracks can lead to an error in the TC intensity.

This is mainly because an inaccurate TC representation experiences different ocean-atmospheric conditions from the observation. As a result, the TC intensity will differ. In our analysis, the TC track error for the different algorithms is calculated only for those TC tracks which are Hits that is detected by the algorithm in the reanalysis and are also present in the observation. For CNRM ~49% of the TC track points have an error of less than 50 km (Figure 8a) and ~83% have error of less than 100 km. Whereas, UZ performs slightly better, with ~54% of track points having error below 50 km and approximately 86% falling within 100 km. The skill of OWZ is relatively poor, with only 25% have an error of less than 50 km (Figure 8a). Moreover, there is no major differences in the TC track error between the AS and the BoB for the CNRM and UZ but OWZ shows marked differences (figure 8b and 8c). This indicates that there is not much difference in the track error performance between UZ and CNRM. Additionally, both algorithms demonstrate consistent results across the AS and BoB basins.

Therefore, from all of the above assessment it can be seen that overall CNRM is performing better in capturing the TCs in the NIO during the post-monsoon season. Due to the highest skill of the CNRM algorithm, we further carried out an in-depth assessment of the atmospheric structure of the FA, Hit and Missed TCs. Previous, studies have shown that the FA by the trackers can arise due to moist processes e.g., convection which may cause a tropospheric column heating along with the generation of a surface low that is falsely detected by the tracker (Bourdin et al., 2022). In order to identify vertical temperature profile of FA, Hits and Missed TC we computed the temperature anomaly at the TC center with respect to the TC surroundings (Figure 9). The Hits consistently show strong warm-core characteristics across all three domains NIO, and the sub-basins AS and BoB. The temperature anomalies increase with height and peak between 400–300 hPa, indicating structurally mature systems. For the systems which are falsely detected by CNRM as TCs, also have a significant warm core profile with the temperature anomaly difference between 300 hPa and 850 hPa less than 1°C and the summation of temperature anomaly at 700 hPa, 500 hPa and 300 hPa exceeds 1°C (Figure 9). Due to this warm structure, these systems are falsely detected as TCs. Whereas, the systems which are Missed have a cold core at 850 hPa and is colder than the Hit and FA. Also, as discussed earlier, the systems which are missed have shorter duration with an average lifespan of only 37.4 hours as compared to Hits which have an average lifespan of 95.6 hours.

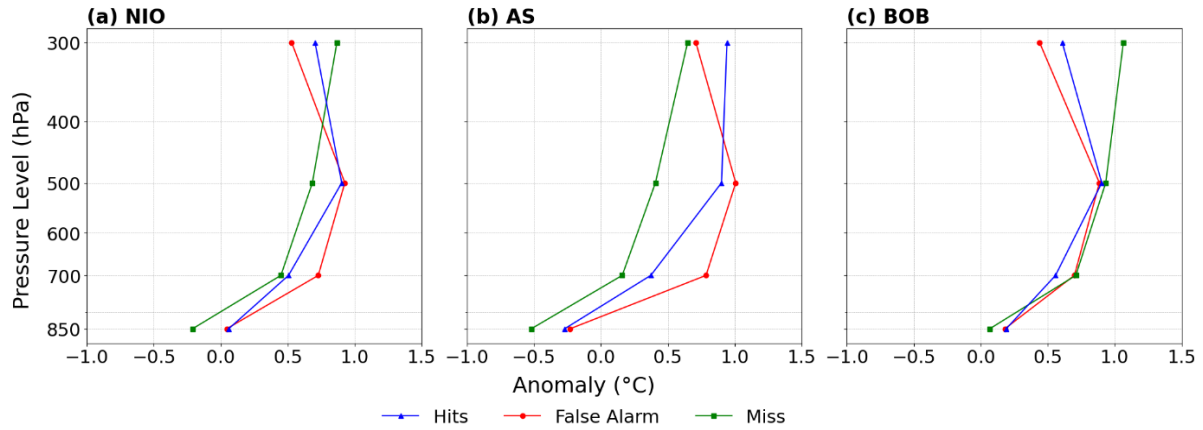


Figure 9. Vertical profiles of temperature anomalies with respect surrounding for the systems classified as Hits (blue), False Alarms (red), and Misses (green) by CNRM algorithm over north Indian Ocean (NIO), Arabian Sea (AS) and Bay of Bengal (BOB).

In addition, it is important to note that the probability of detection (POD) of the CNRM algorithm is higher over the Bay of Bengal than over the Arabian Sea. This regional difference can be explained by the contrasting vertical thermal structures of the systems in the two basins. As shown in Figure 9, Hit cases over the Bay of Bengal exhibit a stronger and more vertically coherent warm-core structure, with positive temperature anomalies extending consistently from the lower to the upper troposphere. Such a structure more effectively satisfies the warm-core and vertical consistency criteria employed by the CNRM tracker. In contrast, systems over the Arabian Sea—particularly those that are missed—tend to exhibit weaker low-level warming and larger vertical variability, making them more likely to fail the thermal and dynamical thresholds required for detection. These differences in vertical structure between the two basins likely explain the relatively higher POD of CNRM over the Bay of Bengal compared to the Arabian Sea.

4. Discussion and Conclusion

In the recent past, multiple studies have analysed the impact of large-scale and local ocean-atmosphere teleconnection and its impact on TC characteristics (Maloney & Hartmann, 2000a, 2000b) using reanalysis products. Accurately representing TCs in reanalysis data is essential for understanding TC dynamics and precisely determining the processes that govern changes in TC activity. However, there is currently no universally accepted methodology for detecting TC genesis and tracking its evolution in reanalysis data or climate models. Consequently,

conclusions drawn from such studies can be influenced by the choice of TC tracking methodology and the thresholds used to identify TCs.

In this study we have utilized the ERA5 reanalysis and evaluated the skill of four TC detection and tracking algorithms to understand the best algorithm which can realistically capture the TC frequency and its track in the NIO during the post-monsoon season. Our analysis shows that in this basin, the CNRM algorithm has the best skill in capturing the TC frequency and track distribution. Although the UZ algorithm has the least error in TC frequency, it fails to capture the bimodal peak in TC frequency and shows a constant TC frequency from April–December (Figure 10). Thus, UZ has poor skill in capturing the bimodal nature of TC in the NIO. Further, analysis shows that the POD is close to 80% for CNRM, which is the highest among all. Furthermore, the direct track error distribution indicates no substantial difference between the performances of the CNRM and UZ algorithms.

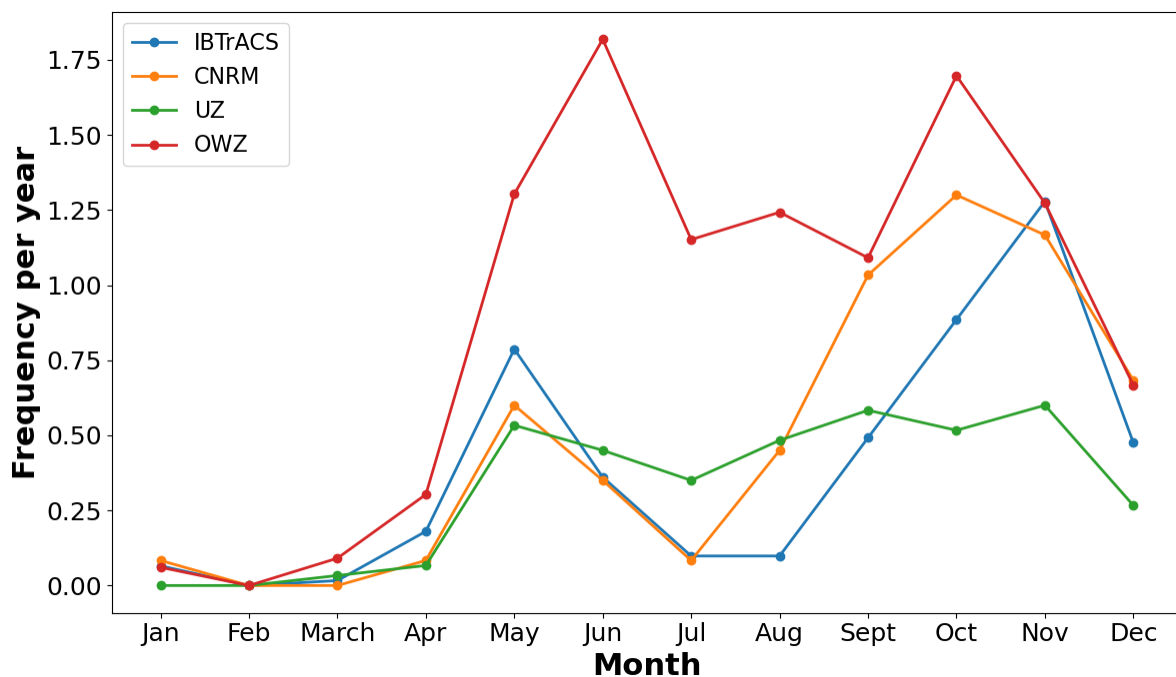


Figure 10. Monthly distribution of Tropical Cyclone frequency/year in the north Indian Ocean for observations (IBTrACS, blue) and in ERA5 using CNRM (orange), UZ (green) and OWZ (red) tracking algorithms for the period 1990–2022.

Additionally, we found that the TRACK algorithm does not incorporate any wind speed-based threshold in its TC detection methodology, relying primarily on relative vorticity and the presence of a warm core. The Bay of Bengal is prone to frequent low-pressure systems that do not intensify into tropical cyclones, as well as strong convective activity during active phases of the Madden–Julian Oscillation, both of which can generate enhanced low-level

vorticity. Previous studies have shown that such monsoon low-pressure systems and MJO-related convective bursts can produce vorticity values exceeding commonly used detection thresholds (Hurley and Boos, 2014). As a result, these weak and short-lived systems may be falsely identified as potential TCs by the TRACK algorithm, leading to an overestimation of TC frequency. We further verified that this overestimation is not due to repeated detection of the same TC, but rather arises from the detection of these non-intensifying systems. Finally, the OWZ does not include a warm-core criterion for TC detection. Since the warm core is a crucial parameter for identifying TCs, its absence may contribute to only 60% POD of TCs and a higher Missing rate in the NIO. This issue also warrants further detailed analysis in the future.

Although CNRM is the best algorithm in capturing the TC frequency and its track distribution, there are few discrepancies. It is over-estimating the TC frequency in the NIO by 20% and ~51% of TC points have a track error of >50 kms. An error in TC track can lead to totally different ocean-atmosphere condition compared to actual conditions which a TC encounters during its lifetime. Thus, it is crucial to minimize the errors in TC detection algorithm and can have an influence on the TC intensity too in the reanalysis. In a recent study it is shown that globally TC intensity is underestimated in ERA5, with strong underestimation of maximum wind speed as compared to the minimum sea-level pressure (Dulac et al., 2024). This underestimation of TC winds is consistent with known limitations of reanalysis data at ~0.25° resolution. The coarser resolution constrains the accurate dynamical representation of the TC inner core (Walsh et al., 2015) resulting in underestimating the intensity (Davis, 2018). However, Dulac et al. (2024) have excluded NIO from their study, therefore it needs to be studied in detail in future which algorithm captures the TC intensity in the NIO in the ERA5 reanalysis.

We also found that while the CNRM algorithm has the least bias in capturing TC duration, it still underestimates TC duration in the NIO during the post-monsoon season by approximately 12% (considering the Hits TCs only). A shorter TC duration in the reanalysis can have significant implications for both the ocean and atmosphere. For instance, reduced TC duration suggests the possibility of TC-induced negative feedback persisting for a shorter period compared to observations. This could lead to a bias in TC-induced sea surface temperature (SST) cooling in the reanalysis, potentially affecting the overall post-TC SST recovery. Research has shown that TC-induced SST cooling impacts oceanic rainfall (Ma et al., 2020), ocean currents (Jeon et al. 2022) and radiative budgets (Pasquero et al., 2021).

Therefore, a bias in TC-induced SST cooling due to a shorter TC lifespan in the reanalysis could lead to biases in several other ocean-atmospheric parameters, with effects persisting for several days to weeks.

This research is only focussed on the post-monsoon season, past research highlights that in the NIO, there is a significant difference in the ocean and atmosphere conditions between the pre-monsoon and the post-monsoon conditions (e.g. (Singh & Roxy, 2022)). Li et al. (2019) also showed that TC genesis features in the BoB differ between these two seasons. This suggests that the skill scores for TC detection by various algorithms may differ between the pre-monsoon and post-monsoon seasons. Therefore, it is necessary to analyze the performance of different TC tracking algorithms separately for the pre-monsoon season. Dulac et al. (2024) show that in the CNRM algorithm, changing the wind speed threshold for TC detection can alter the upper bound of POD of TCs. Additionally, it is found that the wind speed thresholds used for TC detection may vary depending on the resolution of the model or reanalysis data, with higher thresholds typically required for finer resolution models/reanalysis (Murakami & Sugi, 2010; Walsh et al., 2007). Given that the algorithms we have analyzed use different wind speed thresholds to identify TCs, it is important to assess in future studies how these thresholds affect TC frequency and track detection in the NIO.

Overall, the CNRM algorithm demonstrates high accuracy in capturing TC tracks in the NIO. Lastly, for the NIO, CNRM tracking algorithm can be used to detect the future projections of TC activity in the climate models. Its detection thresholds are specifically designed for use with climate model output and have been shown to perform consistently across both historical and future simulations; therefore, substantial systematic bias under warming is not expected, although this remains a general consideration for all fixed-threshold trackers.

Acknowledgement

The authors acknowledge the support provided by the Indian Institute of Tropical Meteorology, Pune, and the Ministry of Earth Sciences, Government of India. Support from the “Deep Ocean Mission” of the Ministry of Earth Sciences, Government of India, is also gratefully acknowledged. The authors sincerely thank the reviewers, Dr. A. K. Sahai, Dr. Medha Deshpande, and Dr. Vishnu S. Nair, for their valuable suggestions and constructive comments, which significantly improved the quality of this report.

References

- Adsul R, Singh VK, Parekh A, Gnanaseelan C. 2026. Near future projections of tropical cyclone tracks over the Bay of Bengal using high resolution CMIP6 models. *Scientific Reports*, 16(1): 5567. <https://doi.org/10.1038/s41598-026-35482-w>.
- Albert, J., Sahoo, B., & Bhaskaran, P. K. (2021). Tropical cyclogenesis identification using eddy detection technique for the Bay of Bengal Basin. *Atmospheric Research*, 260, 105670. <https://doi.org/https://doi.org/10.1016/j.atmosres.2021.105670>
- Ali, A. (1999). Climate change impacts and adaptation assessment in Bangladesh. *Climate Research*, 12.
- Bell, R., Strachan, J., Vidale, P. L., Hodges, K., & Roberts, M. (2013). Response of tropical cyclones to idealized climate change experiments in a global high-resolution coupled general circulation model. *J. Climate*, 26, 7966–7980.
- Bell, S. S., Chand, S. S., Tory, K. J., & Turville, C. (2018). Statistical Assessment of the OWZ Tropical Cyclone Tracking Scheme in ERA-Interim. *Journal of Climate*, 31(6), 2217–2232. <https://doi.org/10.1175/JCLI-D-17-0548.1>
- Bourdin, S., Fromang, S., Dulac, W., Cattiaux, J., & Chauvin, F. (2022). Intercomparison of four algorithms for detecting tropical cyclones using ERA5. *Geoscientific Model Development*, 15(17), 6759–6786. <https://doi.org/10.5194/gmd-15-6759-2022>
- Camargo, S J, & Zebiak, S. E. (2002). Improving the detection and tracking of tropical cyclones in atmospheric general circulation models. *Weather and Forecasting*, 17(6), 1152–1162. [https://doi.org/10.1175/1520-0434\(2002\)017<1152:ITDATO>2.0.CO;2](https://doi.org/10.1175/1520-0434(2002)017<1152:ITDATO>2.0.CO;2)
- Camargo, Suzana J, & Zebiak, S. E. (2002). Improving the Detection and Tracking of Tropical Cyclones in Atmospheric General Circulation Models. *Weather and Forecasting*, 17(6), 1152–1162. [https://doi.org/10.1175/1520-0434\(2002\)017<1152:ITDATO>2.0.CO;2](https://doi.org/10.1175/1520-0434(2002)017<1152:ITDATO>2.0.CO;2)
- Chand, S. S., & Walsh, K. J. E. (2012). Modeling Seasonal Tropical Cyclone Activity in the Fiji Region as a Binary Classification Problem. *Journal of Climate*, 25(14), 5057–5071. <https://doi.org/10.1175/JCLI-D-11-00507.1>
- Chauvin, F., Royer, J. F., & Déqué, M. (2006). Response of hurricane-type vortices to global warming as simulated by ARPEGE-Climat at high resolution. *Climate Dynamics*, 27(4), 377–399. <https://doi.org/10.1007/s00382-006-0135-7>
- Chowdhury, A. M. R., Bhuyia, A. U., Choudhury, A. Y., & Sen, R. (1993). The Bangladesh Cyclone of 1991: Why So Many People Died. *Disasters*, 17(4), 291–304. <https://doi.org/https://doi.org/10.1111/j.1467-7717.1993.tb00503.x>

- Davis, C. A. (2018). Resolving Tropical Cyclone Intensity in Models. *Geophysical Research Letters*, 45(4), 2082–2087. <https://doi.org/10.1002/2017GL076966>
- Deng, E., Xiang, Q., Chan, J. C. L., Dong, Y., Tu, S., Chan, P.-W., & Ni, Y.-Q. (2025). Increasing temporal stability of global tropical cyclone precipitation. *Npj Climate and Atmospheric Science*, 8(1), 11. <https://doi.org/10.1038/s41612-025-00896-2>
- Dulac, W., Cattiaux, J., Chauvin, F., Bourdin, S., & Fromang, S. (2024). Assessing the representation of tropical cyclones in ERA5 with the CNRM tracker. *Climate Dynamics*, 62(1), 223–238. <https://doi.org/10.1007/s00382-023-06902-8>
- Emanuel, K. (2005). Increasing destructiveness of tropical cyclones over the past 30 years. *Nature*, 436(7051), 686–688. <https://doi.org/10.1038/nature03906>
- Hersbach, H., Bell, B., Berrisford, P., Hirahara, S., Horányi, A., Muñoz-Sabater, J., et al. (2020). The ERA5 global reanalysis. *Quarterly Journal of the Royal Meteorological Society*, 146(September 2019), 1–51. <https://doi.org/10.1002/qj.3803>
- Hodges, K., Cobb, A., & Vidale, P. L. (2017). How Well Are Tropical Cyclones Represented in Reanalysis Datasets? *Journal of Climate*, 30(14), 5243–5264. <https://doi.org/10.1175/JCLI-D-16-0557.1>
- Hodges, K. I. (1994). A General Method for Tracking Analysis and Its Application to Meteorological Data. *Monthly Weather Review*, 122(11), 2573–2586. [https://doi.org/10.1175/1520-0493\(1994\)122<2573:AGMFTA>2.0.CO;2](https://doi.org/10.1175/1520-0493(1994)122<2573:AGMFTA>2.0.CO;2)
- Hodges, K. I. (1995). Feature Tracking on the Unit Sphere. *Monthly Weather Review*, 123(12), 3458–3465. [https://doi.org/10.1175/1520-0493\(1995\)123<3458:FTOTUS>2.0.CO;2](https://doi.org/10.1175/1520-0493(1995)123<3458:FTOTUS>2.0.CO;2)
- Hodges, K. I. (1999). Adaptive Constraints for Feature Tracking. *Monthly Weather Review*, 127(6), 1362–1373. [https://doi.org/10.1175/1520-0493\(1999\)127<1362:ACFFT>2.0.CO;2](https://doi.org/10.1175/1520-0493(1999)127<1362:ACFFT>2.0.CO;2)
- Horn, M., Walsh, K., Zhao, M., Camargo, S. J., Scoccimarro, E., Murakami, H., et al. (2014). Tracking Scheme Dependence of Simulated Tropical Cyclone Response to Idealized Climate Simulations. *Journal of Climate*, 27(24), 9197–9213. <https://doi.org/10.1175/JCLI-D-14-00200.1>
- Hurley, J. V. & Boos, W. R. A global climatology of monsoon low-pressure systems. *Quarterly Journal of the Royal Meteorological Society* **141**, 1049–1064 (2014). <https://doi.org/10.1002/qj.2447>
- IMD (2021) Cyclone warning in India standard operation procedure. India meteorological department, Ministry of Earth Sciences, India, p 229. Available at https://mausam.imd.gov.in/imd_latest/contents/pdf/cyclone_sop.pdf

- Jeon, C. J., Watts, D. R., Min, H. S., Kim, D. G., Kang, S. K., Moon, I. J., & Park, J.-H. (2022). Weakening of the Kuroshio upstream by cyclonic cold eddies enhanced by the consecutive passages of Typhoons Danas, Wipha, and Francisco (2013). *Frontiers in Marine Science*, 9. <https://doi.org/doi:10.3389/fmars.2022.884768>
- Jin, C.-S., Cha, D.-H., Lee, D.-K., Suh, M.-S., Hong, S.-Y., Kang, H.-S., & Ho, C.-H. (2016). Evaluation of climatological tropical cyclone activity over the western North Pacific in the CORDEX-East Asia multi-RCM simulations. *Climate Dynamics*, 47(3), 765–778. <https://doi.org/10.1007/s00382-015-2869-6>
- Knapp, K. R., Kruk, M. C., Levinson, D. H., Diamond, H. J., Neumann, C. J., & Kenneth R. Knapp, et al. (2010). The International Best Track Archive for Climate Stewardship (IBTrACS). *Bulletin of the American Meteorological Society*, 91(3), 363–376. <https://doi.org/10.1175/2009BAMS2755.1>
- Li, Z., Yu, W., Li, K., Wang, H., & Liu, Y. (2019). Environmental Conditions Modulating Tropical Cyclone Formation over the Bay of Bengal during the Pre-Monsoon Transition Period. *Journal of Climate*, 32(14), 4387–4394. <https://doi.org/10.1175/JCLI-D-18-0620.1>
- Ma, Z., Fei, J., Lin, Y., & Huang, X. (2020). Modulation of Clouds and Rainfall by Tropical Cyclone's Cold Wakes. *Geophysical Research Letters*, 47(17), 1–8. <https://doi.org/10.1029/2020GL088873>
- Maloney, E. D., & Hartmann, D. L. (2000a). Modulation of eastern north Pacific Hurricanes by the Madden-Julian oscillation. *Journal of Climate*, 13(9), 1451–1460. [https://doi.org/10.1175/1520-0442\(2000\)013<1451:MOENPH>2.0.CO;2](https://doi.org/10.1175/1520-0442(2000)013<1451:MOENPH>2.0.CO;2)
- Maloney, E. D., & Hartmann, D. L. (2000b). Modulation of Hurricane Activity in the Gulf of Mexico by the Madden-Julian Oscillation. *Science*, 287(5460), 2002–2004. <https://doi.org/10.1126/science.287.5460.2002>
- Murakami, H. (2014). Tropical cyclones in reanalysis data sets. *Geophysical Research Letters*, 41(6), 2133–2141. <https://doi.org/https://doi.org/10.1002/2014GL059519>
- Murakami, H., & Sugi, M. (2010). Effect of Model Resolution on Tropical Cyclone Climate Projections. *SOLA*, 6, 73–76. <https://doi.org/10.2151/sola.2010-019>
- Murakami, H., Mizuta, R., & Shindo, E. (2012). Future changes in tropical cyclone activity projected by multi-physics and multi-SST ensemble experiments using the 60-km-mesh MRI-AGCM. *Climate Dynamics*, 39(9–10), 2569–2584. <https://doi.org/10.1007/s00382-011-1223-x>
- Murakami, H., Sugi, M., & Kitoh, A. (2014). Future Changes in Tropical Cyclone Activity in

- the North Indian Ocean Projected by the New High-Resolution MRI-AGCM. In R. L. S. Mohanty U.C., Mohapatra M., Singh O.P., Bandyopadhyay B.K., Rathore L.S. (Ed.), *Monitoring and Prediction of Tropical Cyclones in the Indian Ocean and Climate Change* (Vol. 40, pp. 65–71). Dordrecht: Springer Netherlands. https://doi.org/10.1007/978-94-007-7720-0_6
- Oouchi, K., Yoshimura, J., Yoshimura, H., Mizuta, R., Kusunoki, S., & Noda, A. (2006). Tropical Cyclone Climatology in a Global-Warming Climate as Simulated in a 20 km-Mesh Global Atmospheric Model: Frequency and Wind Intensity Analyses. *Journal of the Meteorological Society of Japan. Ser. II*, 84(2), 259–276. <https://doi.org/10.2151/jmsj.84.259>
- Pasquero, C., Desbiolles, F., & Meroni, A. N. (2021). Air-Sea Interactions in the Cold Wakes of Tropical Cyclones. *Geophysical Research Letters*, 48(2), 1–6. <https://doi.org/10.1029/2020GL091185>
- Raavi, P. H., & Walsh, K. J. E. (2020). Sensitivity of Tropical Cyclone Formation to Resolution-Dependent and Independent Tracking Schemes in High-Resolution Climate Model Simulations. *Earth and Space Science*, 7(3), e2019EA000906. <https://doi.org/https://doi.org/10.1029/2019EA000906>
- Rajeevan, M., Srinivasan, J., Niranjan Kumar, K., Gnanaseelan, C., & Ali, M. M. (2013). On the epochal variation of intensity of tropical cyclones in the Arabian Sea. *Atmospheric Science Letters*, 14(4), 249–255. <https://doi.org/10.1002/asl2.447>
- Rathmann, N. M., Yang, S., & Kaas, E. (2014). Tropical cyclones in enhanced resolution CMIP5 experiments. *Climate Dynamics*, 42(3–4), 665–681. <https://doi.org/10.1007/s00382-013-1818-5>
- Rios Gaona, M. F., Villarini, G., Zhang, W., & Vecchi, G. A. (2018). The added value of IMERG in characterizing rainfall in tropical cyclones. *Atmospheric Research*, 209, 95–102. <https://doi.org/https://doi.org/10.1016/j.atmosres.2018.03.008>
- Sahoo, B., & Bhaskaran, P. K. (2016). Assessment on historical cyclone tracks in the Bay of Bengal, east coast of India. *International Journal of Climatology*, 36(1), 95–109. <https://doi.org/10.1002/joc.4331>
- Soccimarro, E., Gualdi, S., & Navarra, A. (2012). Tropical cyclone effects on Arctic Sea ice variability. *Geophysical Research Letters*, 39(17). <https://doi.org/https://doi.org/10.1029/2012GL052987>
- Singh, O. P., Ali Khan, T. M., & Rahman, M. S. (2000). Changes in the frequency of tropical cyclones over the North Indian Ocean. *Meteorology and Atmospheric Physics*, 75(1–2),

11–20. <https://doi.org/10.1007/s007030070011>

- Singh, V. K., & Roxy, M. K. (2022). A review of ocean-atmosphere interactions during tropical cyclones in the north Indian Ocean. *Earth-Science Reviews*, 226, 103967. <https://doi.org/10.1016/j.earscirev.2022.103967>
- Strachan, J., Vidale, P. L., Hodges, K., Roberts, M., & Demory, M.-E. (2013). Investigating Global Tropical Cyclone Activity with a Hierarchy of AGCMs: The Role of Model Resolution. *Journal of Climate*, 26(1), 133–152. <https://doi.org/10.1175/JCLI-D-12-00012.1>
- Taylor, K. E. (2001). Summarizing multiple aspects of model performance in a single diagram. *Journal of Geophysical Research: Atmospheres*, 106(D7), 7183–7192. <https://doi.org/https://doi.org/10.1029/2000JD900719>
- Tory, K. J., Chand, S. S., Dare, R. A., & McBride, J. L. (2013). An Assessment of a Model-, Grid-, and Basin-Independent Tropical Cyclone Detection Scheme in Selected CMIP3 Global Climate Models. *Journal of Climate*, 26(15), 5508–5522. <https://doi.org/10.1175/JCLI-D-12-00511.1>
- Tory, K. J., Chand, S. S., McBride, J. L., Ye, H., & Dare, R. A. (2013). Projected Changes in Late-Twenty-First-Century Tropical Cyclone Frequency in 13 Coupled Climate Models from Phase 5 of the Coupled Model Intercomparison Project. *Journal of Climate*, 26(24), 9946–9959. <https://doi.org/10.1175/JCLI-D-13-00010.1>
- Truchelut, R. E., Hart, R. E., & Luthman, B. (2013). Global Identification of Previously Undetected Pre-Satellite-Era Tropical Cyclone Candidates in NOAA/CIRES Twentieth-Century Reanalysis Data. *Journal of Applied Meteorology and Climatology*, 52(10), 2243–2259. <https://doi.org/10.1175/JAMC-D-12-0276.1>
- Ullrich, P. A., Zarzycki, C. M., McClenny, E. E., Pinheiro, M. C., Stansfield, A. M., & Reed, K. A. (2021). TempestExtremes v2.1: a community framework for feature detection, tracking, and analysis in large datasets. *Geoscientific Model Development*, 14(8), 5023–5048. <https://doi.org/10.5194/gmd-14-5023-2021>
- Walsh, K J E, Fiorino, M., Landsea, C. W., & McInnes, K. L. (2007). Objectively Determined Resolution-Dependent Threshold Criteria for the Detection of Tropical Cyclones in Climate Models and Reanalyses. *Journal of Climate*, 20(10), 2307–2314. <https://doi.org/10.1175/JCLI4074.1>
- Walsh, Kevin J E, Camargo, S. J., Vecchi, G. A., Daloz, A. S., Elsner, J., Emanuel, K., et al. (2015). Hurricanes and Climate: The U.S. CLIVAR Working Group on Hurricanes. *Bulletin of the American Meteorological Society*, 96(6), 997–1017.

<https://doi.org/https://doi.org/10.1175/BAMS-D-13-00242.1>

Zarzycki, C. M., & Ullrich, P. A. (2017). Assessing sensitivities in algorithmic detection of tropical cyclones in climate data. *Geophysical Research Letters*, *44*(2), 1141–1149.

<https://doi.org/https://doi.org/10.1002/2016GL071606>

Zarzycki, C. M., Ullrich, P. A., & Reed, K. A. (2021). Metrics for Evaluating Tropical Cyclones in Climate Data. *Journal of Applied Meteorology and Climatology*, *60*(5), 643–660. <https://doi.org/10.1175/JAMC-D-20-0149.1>

Zhou, X., Lu, R., & Chen, G. (2018). Impact of Interannual Variation of Synoptic Disturbances on the Tracks and Landfalls of Tropical Cyclones over the Western North Pacific, *35*(December), 1469–1477.